Applied Physics Letters

Platinum composition dependence of spin-orbit torque in $(Fe_{0.8}Mn_{0.2})_{1-x}Pt_x$ single-layer ferromagnet

Cite as: Appl. Phys. Lett. **117**, 172402 (2020); https://doi.org/10.1063/5.0023957
Submitted: 03 August 2020 . Accepted: 09 October 2020 . Published Online: 26 October 2020

Ziyan Luo, Ling Lu, Hang Xie, Yanjun Xu, Xin Chen, Abhishek Talapatra, Adekunle Olusola Adeyeye, Younan Hua, Xiaomin Li, and Yihong Wu

Applied Physics Letters ARTICLE scitation.org/journal/apl

Platinum composition dependence of spin-orbit torque in $(Fe_{0.8}Mn_{0.2})_{1-x}Pt_x$ single-layer ferromagnet

Cite as: Appl. Phys. Lett. **117**, 172402 (2020); doi: 10.1063/5.0023957
Submitted: 3 August 2020 · Accepted: 9 October 2020 ·
Published Online: 26 October 2020

Ziyan Luo,[1,2] Ling Lu,[1,3] Hang Xie,[1] Yanjun Xu,[1] Xin Chen,[1] Abhishek Talapatra,[1] Adekunle Olusola Adeyeye,[1,4] Younan Hua,[3] Xiaomin Li,[3] and Yihong Wu[1,a)]

AFFILIATIONS

[1]Department of Electrical and Computer Engineering, National University of Singapore, 4 Engineering Drive 3, Singapore 117583, Singapore
[2]School of Physics and Electronics, Central South University, Changsha, 410083, China
[3]WinTech Nano-Technology Services Pte Ltd. 10 Science Park Road #03-26, The Alpha, Science Park II, Singapore 117684
[4]Department of Physics, Durham University, South Road, Durham DH1 3LE, United Kingdom

[a)]Author to whom correspondence should be addressed: elewuyh@nus.edu.sg

ABSTRACT

We have investigated the effect of the Pt composition on the spin–orbit torque in a $(Fe_{0.8}Mn_{0.2})_{1-x}Pt_x$ single-layer ferromagnet. We observed that while the field-like torque decreases and even reverses sign with increasing the Pt composition, the damping-like torque increases monotonically and reaches 0.99 $Oe/(10^{10}\ A/m^2)$ in a single-layer $(Fe_{0.8}Mn_{0.2})_{0.52}Pt_{0.48}$ film. The results corroborate the anomalous Hall effect and surface spin rotation model presented previously, and the relative ratio between the damping-like and field-like torques can be qualitatively understood as the relative phase change in spin-conserving and spin-flip scattering.

Interconversion between spin and charge current has been widely studied in a variety of heavy metal (HM)/ferromagnet (FM) heterostructures. When a charge current passes through a HM/FM bilayer, it induces spin–orbit torques (SOTs) acting on the magnetization of the FM layer due to either the spin Hall effect (SHE)[1–4] of the HM or the Rashba–Edelstein effect (REE) at the interface.[5–7] In addition to the SHE and REE, there might be other mechanisms of interfacial origin, which are still under debate.[8–10] In general, the current-induced torques can be categorized into two main types, termed as damping-like (DL) $[\hat{\tau}_{DL} \propto \hat{m} \times (\hat{m} \times \hat{\sigma})]$ and field-like (FL) $[\hat{\tau}_{FL} \propto (\hat{m} \times \hat{\sigma})]$ torque, respectively, where $\hat{\sigma}$ is the spin polarization direction and $\hat{m}$ the magnetization direction of the FM.[11–13] The FL torque is due to the exchange interaction between the lattice or non-equilibrium spins with the local magnetization, whereas the DL torque is through angular momentum transfer. In addition to the HM/FM bilayers, recently there is also growing interest in spin-charge interconversion in a single layer FM. When a charge current passes a FM, it becomes polarized due to the exchange interaction between the itinerant electrons and the local magnetic moment. When these polarized electrons are scattered by the scattering centers with large spin–orbit coupling (SOC) or by the virtual magnetic field due to the Berry curvature, it leads to both transverse charge and spin currents, which is commonly known as the anomalous Hall effect (AHE).[14] Due to the strong exchange coupling, the spin polarization of the transverse spin current is believed to be aligned with the local magnetization direction (or longitudinal spin polarization). Although this provides a convenient way to control the spin polarization direction using an external field,[15–20] it also means that the AHE-generated non-equilibrium spins in a single layer FM are unable to exert a torque on its own magnetization.[15,16]

Recently, we have demonstrated that a different scenario emerges in the vicinity of the surface of a thin FeMn layer, particularly within the range of spin relaxation lengths.[21] Due to relatively strong SOC in FeMn, the polarization of AHE-generated spins rotates away from the initial direction after being scattered from the SOC scattering center. The subsequent backflow of these non-equilibrium spins exerts a torque on the local magnetization. Considering both the top and bottom surfaces of the single-layer ferromagnet, the net torque from the non-equilibrium spins may be written as[22]

$$\hat{\tau}_{net} = \frac{(P_s + P_\sigma)}{2}[S + (1-T)\hat{m}\cdot\hat{n}]\,\hat{m}\times(\hat{m}\times\hat{n}) + U\hat{m}\times\hat{n}, \quad (1)$$

where $P_s = (N_\uparrow - N_\downarrow)/(N_\uparrow + N_\downarrow)$, $P_\sigma \equiv (\sigma_\uparrow - \sigma_\downarrow)/(\sigma_\uparrow + \sigma_\downarrow)$, with $N_\uparrow(N_\downarrow)$ the electron density and $\sigma_\uparrow(\sigma_\downarrow)$ the conductivity of spin-up and spin-down electrons, S, T, and U are the scattering coefficients, $\hat{m}$ is the magnetization direction, and $\hat{n} = \hat{k} \times \hat{k}'$ is the normal vector of the scattering plane, with $\hat{k}$ ($\hat{k}'$) the moving direction of the electron before (after) scattering. For a film with in-plane magnetic anisotropy, the first term is equivalent to the DL torque (though it is modulated partially by the $\hat{m} \cdot \hat{n}$ term), while the second term is equivalent to a FL torque observed in HM/FM bilayers. According to Kessler,[23] S and U represent the spin rotation terms due to spin-flip scattering, whereas T denotes the difference between spin-flip and spin-conserved scattering amplitudes, and $S^2 + T^2 + U^2 = 1$. In the previous work on $Fe_{0.8}Mn_{0.2}$, we only observed the FL term, and the DL torque was estimated to be negligible.[21] This could be due to two reasons: (1) the method we used to evaluate the SOT is not sensitive to DL and (2) the DL torque in $Fe_{0.8}Mn_{0.2}$ is small. Regarding (1), we have previously used the Wheatstone bridge[21,24] to evaluate the FL torque and the results are in good agreement with the values obtained from the second-order planar Hall effect measurement.[25–27] The Wheatstone bridge method provides superior signal quality as it effectively suppresses the thermal drift. It is particularly effective in evaluating the FL effective field in the FM with in-plane anisotropy as demonstrated in our previous work on spin Hall magnetoresistance (SMR) sensors.[28–30] The signal related to the DL torque is negligible as magnetization is mostly in-plane. Although one can extend the technique to measure the DL torque by applying a large out-of-plane field,[31] its sensitivity is around two orders of magnitude smaller, which adversely compensates the advantage of the bridge method. As for the second possibility, i.e., the DL torque is small in $Fe_{0.8}Mn_{0.2}$. This is highly possible as S and U both originate from the same source of spin-flip scattering; therefore, when U is large, S should be small.

In view of the above, in this work, we investigated systematically how the DL and FL torques vary in $(Fe_{0.8}Mn_{0.2})_{1-x}Pt_x$ (hereafter, we refer it to as FeMnPt) with the Pt composition. This is stimulated by our previous findings that FeMnPt exhibits a larger AHE compared to FeMn.[32] Due to the low-sensitivity of the Wheatstone bridge method to DL torque for films with in-plane anisotropy, here we use the harmonic Hall measurement for measuring both the DL and FL torques. It is found that the DL SOT efficiency increases with the Pt concentration, while the FL SOT efficiency decreases accordingly. A damping-like SOT efficiency of 0.99 Oe/(10^{10} A/m^2) is obtained in the sample with the highest Pt concentration ($x = 0.48$), while the field-like SOT efficiency is around 0.09 Oe/(10^{10} A/m^2), which is one order of magnitude smaller than that of DL SOT. The trend of FL and DL SOT corroborates the AHE-origin of both phenomena in combination with surface spin rotation.

The MgO(2)/$(Fe_{0.8}Mn_{0.2})_{1-x}Pt_x(d)$ samples (with MgO as the capping layer) used for the harmonic Hall measurement are deposited directly on the SiO_2/Si substrate, with the Pt power ranging from 0 W ($x = 0$) to 35 W ($x = 0.48$) and d ranging from 4 to 10 nm. Here, the number inside the parentheses indicates the layer thickness in nm. All the layers are prepared by dc magnetron sputtering with a base pressure of 2×10^{-8} Torr and a working pressure of 3×10^{-3} Torr, respectively. The Hall devices are formed using combined techniques of photolithography and lift-off. During the electrical measurements, an ac current is supplied by a Keithley 6221 current source, and the harmonic signal is recorded by a Zurich 500 kHz MFLI lock-in amplifier. The dc output voltage is captured by a Keithley 2182 A nanovoltmeter (for the dc Hall resistance measurement). All the measurements are performed at room temperature (300 K) using a Quantum Design Versalab Physical Property Measurement System.

Figure 1(a) describes the geometry of the harmonic Hall measurement, where the devices are patterned into Hall bars with dimensions of 100 μm (width) × 500 μm (length). Here, φ_m and θ_m refer to the azimuthal and polar angle of the magnetization $\hat{m}$, respectively. When an ac current $I_0 \sin \omega t$ flows along the x direction, the first order expression for the Hall resistance can be written as

$$R_H^\omega = R_{AHE} \cos\theta_m + R_{PHE} \sin^2\theta_m \sin 2\varphi_m, \tag{2}$$

where R_{AHE} and R_{PHE} refer to the anomalous Hall resistance and planar Hall resistance, respectively. Considering the small changes in θ_m and φ_m induced by the SOT effective field, the related second order signal is approximately given by[33–35]

$$\begin{aligned} R_{SOT}^{2\omega} &= \frac{1}{2}\left(R_{AHE}\frac{d\cos\theta_m}{d\theta_m}\Delta\theta_m + R_{PHE}\sin 2\varphi_m \frac{d\sin^2\theta_m}{d\theta_m}\Delta\theta_m \right. \\ &\quad \left. + R_{PHE}\sin^2\theta_m \frac{d\sin 2\varphi_m}{d\varphi_m}\Delta\varphi_m\right) \\ &= \frac{1}{2}(-R_{AHE}\sin\theta_m\Delta\theta_m + R_{PHE}\sin 2\varphi_m \sin 2\theta_m \Delta\theta_m \\ &\quad + 2R_{PHE}\sin^2\theta_m \cos 2\varphi_m \Delta\varphi_m), \end{aligned} \tag{3}$$

where $\Delta\theta_m$ and $\Delta\varphi_m$ are the current-induced small variations and can be estimated using the first-order approximation,[21,33] namely, $\Delta\theta_m \approx \frac{H_I^\theta}{(H_{ex}+H_d)}$ and $\Delta\varphi_m \approx \frac{H_I^\varphi}{H_{ex}}$; here, $H_I^\theta(H_I^\varphi)$ is the $\theta(\varphi)$ component of the current-induced effective field (H_I) and H_d is the out-of-plane demagnetizing field. According to the measurement geometry, θ_m is

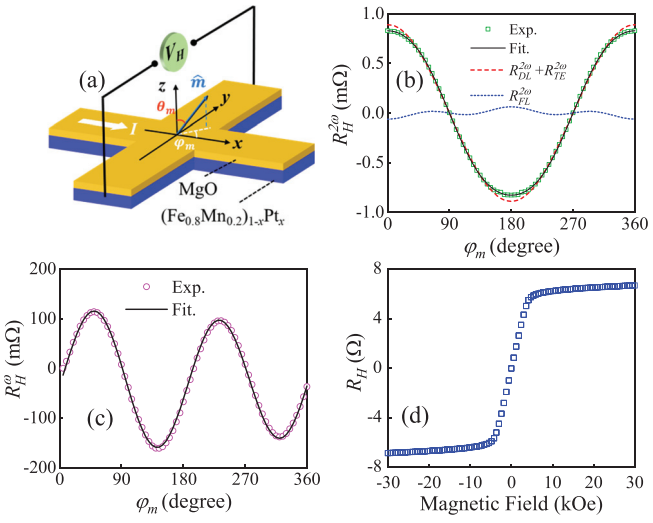

FIG. 1. (a) Schematic illustration of the harmonic Hall measurement. (b) Experimental (symbol) and fitting (sold line) results of $R_H^{2\omega}$ vs φ_m at $H_{ex} = 500$ Oe. Dashed and dotted lines refer to $(R_{DL}^{2\omega} + R_{TE}^{2\omega})$ and $R_{FL}^{2\omega}$, respectively. (c) Experimental (symbol) and fitting (solid line) results of first harmonic resistance (R_H^ω) as a function of φ_m. (d) Hall resistance R_H measured with a dc current and an out-of-plane external magnetic field.

nearly $\pi/2$, and the induced $\Delta\theta_m$, if any, should be much smaller than θ_m as $H_I^\theta \ll H_d$. As demonstrated in Eq. (1), DL torque has the form of $[S + (1-T)\hat{m}\cdot\hat{n}]\,\hat{m}\times(\hat{m}\times\hat{n})$. Since the effective field is proportional to current density, it can be further written as $H_I^\theta = -\alpha_{DL} j_{0\_rms}\cos\varphi_m + \alpha'_{DL} j_{0\_rms}\cos\varphi_m \sin\varphi_m$, where α_{DL} and α'_{DL} are the DL SOT efficiency corresponding to the S and T related terms in Eq. (1), respectively. $j_{0\_rms} = I_0/(\sqrt{2}wd)$ is the rms amplitude of the applied ac current density, with w being the width and d the thickness of the Hall structure. Similarly, for the FL effective field, we have $H_I^\varphi = \alpha_{FL} j_{0\_rms}\cos\varphi_m$, where α_{FL} is the FL SOT efficiency corresponding to the U related term in Eq. (1). In addition to the current-induced SOT effective field, the current injection in FM layers creates a perpendicular temperature gradient due to Joule heating and asymmetric heat dissipation toward the air and substrate side.[33] Therefore, we have to include the thermoelectric (TE) contribution $I_0\alpha_{TE}\nabla T_z\cos\varphi_m$, with α_{TE} being the effective coefficient that accounts for both the anomalous Nernst effect (ANE) and the spin Seebeck effect (SSE) and ∇T_z the temperature gradient. Therefore, the total harmonic Hall resistance can be written as

$$R_H^{2\omega} = \frac{1}{2}\left[R_{AHE}\frac{j_{0\_rms}}{H_{ex}+H_d}\left(\alpha_{DL}\cos\varphi_m + \alpha'_{DL}\cos\varphi_m\sin\varphi_m\right) + R_{PHE}\frac{\alpha_{FL} j_{0\_rms}}{H_{ex}}\left(\cos\varphi_m + \cos 3\varphi_m\right) + I_0\alpha_{TE}\nabla T_z\cos\varphi_m\right]. \quad (4)$$

According to the above equation, the second term (hereafter, $R_{FL}^{2\omega}$) vanishes at $\varphi_m = 45°$, 135°, 225°, and 315°, while the first term ($R_{DL}^{2\omega}$) and third term ($R_{TE}^{2\omega}$) do not. Therefore, we can separate $R_{DL}^{2\omega}$ and $R_{FL}^{2\omega}$ by fitting a cosine-like curve that passes through these four points (as we will show shortly, the α'_{DL} related DL term is negligibly small). The DL and TE contributions can be further separated by performing measurements at different external fields as $R_{DL}^{2\omega}$ depends on the magnetic field but $R_{TE}^{2\omega}$ does not.

We first perform the harmonic Hall measurement by applying an external field (H_{ex}) in the xy plane and record the first and second harmonic resistance simultaneously. A typical second order harmonic signal ($R_H^{2\omega}$) of the sample structure MgO(2)/$(Fe_{0.8}Mn_{0.2})_{0.52}Pt_{0.48}$(6) measured at $H_{ex} = 500$ Oe is shown in Fig. 1(b). The circle indicates the experimental results and the solid-line is the overall fitting based on Eq. (4) excluding the α'_{DL} related term, which has a different angular dependence. The good agreement between fitting and experimental results without the α'_{DL} term suggests that the DL torque is dominated by the $\hat{m}\times(\hat{m}\times\hat{n})$ symmetry and the $\hat{m}\cdot\hat{n}$ containing term in Eq. (1) is negligible. The dashed and dotted lines correspond to the $(R_{DL}^{2\omega} + R_{TE}^{2\omega})$ and the $R_{FL}^{2\omega}$ components, respectively. The Oersted field effect can be ignored in a single-layer film. Figure 1(c) shows R_H^ω as a function of φ_m, where a typical sin $2\varphi_m$ dependence is obtained, as expected from Eq. (2). The good fitting to Eq. (2) (solid curve) indicates that the magnetization almost follows the direction of the external field, ensuring the validity of the first-order approximation for calculating the SOT effect. Through the fitting, we can also extract R_{PHE}, which is around 130 $m\Omega$. Figure 1(d) shows the anomalous Hall resistance measured at 1 mA with the field sweeping from −30 kOe to 30 kOe, from which we obtain $R_{AHE} \approx 6.29\ \Omega$. We extrapolate linear fitting of R_H vs magnetic field at both low and high fields, and the intercept of two extrapolated lines gives a rough estimation of $H_d \approx 4.25$ kOe.[35]

We now turn to the external field dependence of the second harmonic signal by varying the field from 300 Oe to 5000 Oe. Figure 2(a) shows a plot of $(R_{DL}^{2\omega} + R_{TE}^{2\omega})$ as a function of $1/(H_{ext}+H_d)$, with the slope proportional to the DL efficiency and y-axis intercept, around 0.18 mΩ, proportional to the thermoelectric contribution. With R_{AHE} and H_d obtained above and a rms current density $j_{0\_rms} \approx 1.06\times10^{10}$ A/m^2, the DL efficiency can be calculated as $\alpha_{DL} \approx 0.99\ \text{Oe}/(10^{10}\ \text{A/m}^2)$. Similarly, Fig. 2(b) indicates that $R_{FL}^{2\omega}$ is linearly proportional to the inverse of the external magnetic field, with the slope proportional to the FL SOT efficiency. Using $R_{PHE} \approx 130$ mΩ, the FL efficiency is calculated as $\alpha_{FL} \approx 0.09\ \text{Oe}/(10^{10}\ \text{A/m}^2)$. Figure 2(c) plots $R_{DL}^{2\omega}$ and $R_{FL}^{2\omega}$ as a function of rms current density at $H_{ex} = 500$ Oe. As expected, an almost linear dependence is observed, which correlates well with Eq. (4). It is interesting to note that α_{DL} is more than one order of magnitude larger than α_{FL} in MgO(2)/$(Fe_{0.8}Mn_{0.2})_{0.52}Pt_{0.48}$(6), which is in sharp contrast to our previous finding on MgO(2)/$Fe_{0.8}Mn_{0.2}$(6), in which α_{FL} is $0.11\ \text{Oe}/(10^{10}\ \text{A/m}^2)$ while α_{DL} is negligibly small.[21]

To shed light on the role of Pt, we compare the harmonic Hall signal of MgO(2)/$(Fe_{0.8}Mn_{0.2})_{1-x}Pt_x$(6) at varying deposition powers of Pt ranging from 0 W ($x=0$) to 35 W ($x=0.48$). Figure 3(a) shows the $R_H^{2\omega}$ measured at $H_{ex} = 500$ Oe for samples with different Pt concentrations. Distinct behaviors are observed for different samples. For samples with $x=0.33$ and $x=0.48$, an obvious cos φ_m dependence is recognized with a slight deviation which comes from the FL

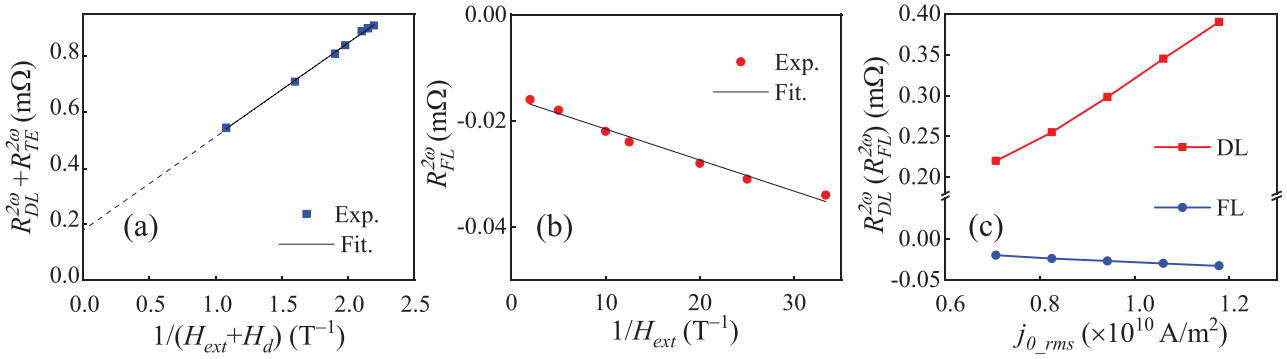

FIG. 2. (a) $(R_{DL}^{2\omega} + R_{TE}^{2\omega})$ as a function of $1/(H_{ext}+H_d)$. (b) $R_{FL}^{2\omega}$ as a function of $1/H_{ext}$. (c) $R_{DL}^{2\omega}(R_{FL}^{2\omega})$ as a function of rms current density at $H_{ex} = 500$ Oe.

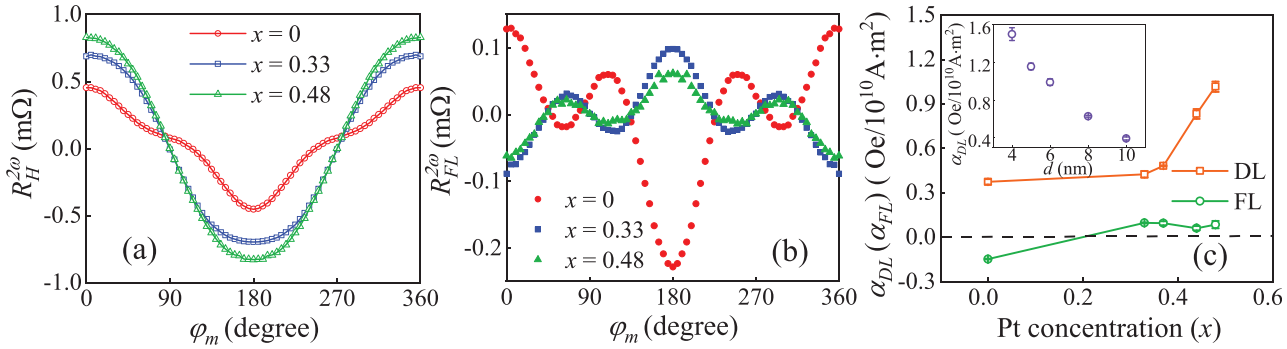

FIG. 3. (a) $R_H^{2\omega}$ and (b) $R_{FL}^{2\omega}$ as a function of φ_m for samples MgO(2)/$(Fe_{0.8}Mn_{0.2})_{1-x}Pt_x$(6) with $x = 0$, $x = 0.33$, and $x = 0.48$. (c) α_{DL} and α_{FL} as a function of Pt concentration in MgO(2)/$(Fe_{0.8}Mn_{0.2})_{1-x}Pt_x$(6). The inset of (c) shows the thickness dependence of DL SOT efficiency in $(Fe_{0.8}Mn_{0.2})_{0.52}Pt_{0.48}$. Error bars indicate the fitting error in each device.

contribution $(\cos\varphi_m + \cos 3\varphi_m)$. For sample without Pt $(x = 0)$, however, the overall shape deviates significantly from $\cos\varphi_m$ due to the large FL component. By fitting, we can remove $(R_{DL}^{2\omega} + R_{TE}^{2\omega})$ from the total signal and extract $R_{FL}^{2\omega}$ as a function of φ_m, as shown in Fig. 3(b). It is clear that, in addition to a large magnitude, α_{FL} also has an opposite sign in the $x = 0$ sample as compared to α_{FL} in the other two samples. Figure 3(c) shows α_{DL} and α_{FL} as a function of Pt concentration (note: due to the constraint of experimental setup, the smallest x we could obtain is around 0.33). As can be seen from the figure, with the increasing Pt concentration, α_{DL} increases slowly at a low Pt composition and it increases rapidly when x exceeds 0.4. On the other hand, α_{FL} is negative for the $x = 0$ sample and positive for all other samples. The sign change has been confirmed by repeating the experiments, but it is difficult to determine the exact Pt composition at which α_{FL} changes the sign. After it reaches a broad maximum around $x = 0.35$, α_{FL} decreases slightly with a further increase in Pt composition. To gain further insight into the origin of DL SOT in single layer $(Fe_{0.8}Mn_{0.2})_{0.52}Pt_{0.48}$, we investigate the thickness dependence of DL SOT efficiency in MgO(2)/$(Fe_{0.8}Mn_{0.2})_{0.52}Pt_{0.48}(d)$ with d varying from 4 nm to 10 nm at a fixed current density of $j_{0\_rms} = 1.06 \times 10^{10}$ A/m^2. As shown in the inset of Fig. 3(c), α_{DL} decays monotonically with the thickness, similar to the trend of thickness-dependence of FL torque reported previously.[21] Both results suggest the surface origin of the AHE-induced SOT.

The above results can be qualitatively understood by examining the S, T, and U parameters in Eq. (1). According to Kessler,[23] S, T, and U can be expressed as

$$S = i\frac{fg^* - f^*g}{|f|^2 + |g|^2}, \quad T = \frac{|f|^2 - |g|^2}{|f|^2 + |g|^2}, \quad U = \frac{fg^* + f^*g}{|f|^2 + |g|^2}, \tag{5}$$

where f and g denote the scattering coefficients of spin-conserving and spin-flipping scattering, respectively. After some algebra, we can obtain $\frac{S}{U} = \frac{\tan\varphi_g - \tan\varphi_f}{1 + \tan\varphi_g \tan\varphi_f}$, where φ_g and φ_f are the phases of g and f, respectively. We have demonstrated previously that by doping Pt into FeMn, a larger anomalous Hall angle (θ_{AHE}) can be obtained.[32] Theoretical studies on the AHE in FeMnPt are not available, but according to Zhang *et al.*, spin-flip transition plays an important role in determining the anomalous Hall conductivity in the FePt alloy.[36] If the same also applies to FeMnPt, we can assume that the doping of Pt could have led to a change in the relative phase of g and f, which gives a large S/U ratio, or equivalently a large DL/FL torque ratio [see Eq. (1)], and even reverses the sign depending on the value of φ_g and φ_f. As $S^2 + T^2 + U^2 = 1$,[23] when DL torque increases, the FL would decrease. This qualitatively explains the trend in Fig. 3(c), though further theoretical studies are required to quantify the DL and FL torques in single-layer FeMnPt, which is out of the scope of this work.

Before we conclude, we comment on possible alternative explanations of the experimental results. Recent theoretical studies showed that not only the longitudinal spin polarization but transverse spin components can also persist in the spin current generated by a charge current inside the FM itself.[36–41] Symmetry analysis suggests that when a charge current flows in the x direction, a spin current flowing in the z-direction possesses polarization components not only in the y-direction but also in the z-direction (when $\hat{m} \parallel \hat{x}$) and x-direction (when $\hat{m} \parallel \hat{z}$).[39] The y-polarized component is the same as the spin current generated in non-magnetic metal (NM) by the SHE as it is independent of the magnetization direction (or is even with respect to the magnetization), whereas the x- and z-polarized components are odd with respect to the magnetization. The latter is also called the transverse spin Hall effect (TSHE) or the magnetic spin Hall effect.[42] Experimentally, the magnetization-independent inverse spin Hall effect (ISHE) has been observed in Co, which is attributed to an intrinsic effect due to the electronic band structure.[43] A similar effect has also been observed in Permalloy together with a magnetization-dependent component, which is termed as the magnetization-dependent inverse anomalous spin Hall effect (ASHE).[44,45] There was also a report that the ISHE in Permalloy is strongly dependent on the spin orientation.[46] Although the transversely polarized spin current can exert torque on the FM magnetization, in principle, the net effect is negligibly small for a thin film with uniform magnetization.[47] Very recently, SOT-based magnetization switching has been demonstrated in single-layer $L1_0$ FePt, which is attributed to either naturally formed or intentionally introduced composition gradients.[48,49] Although the composition gradient has been demonstrated previously as an effective way to break inversion symmetry in the THz emission study of FeMnPt,[50] the switching mechanism in $L1_0$ FePt remains unclear as the polarization of spin current in $L1_0$ FePt was reported to be dominantly

in the local magnetization direction.[19] Although we do not exclude all these alternative explanations, we strongly believe what we have observed originate from the surface effect instead of a bulk mechanism.

In summary, we have investigated the effect of the Pt composition on the spin–orbit torque in single-layer $(Fe_{0.8}Mn_{0.2})_{1-x}Pt_x$ films. We found that the DL torque increases, whereas the FL torque decreases with the Pt concentration. The relative strength of DL and FL torques is determined by the nature of the scattering process, which in turn depends on the host material and scattering centers. The thickness dependence affirms the surface origin of the torque observed. Although we have employed FeMnPt in this study, we believe it should be a general phenomenon in all FMs with a large AHE. We hope our findings will spur further research and enhance the understanding of spin-charge interconversion in single-layer ferromagnets.

Y.W. would like to acknowledge support from the Ministry of Education, Singapore, under its Tier 2 Grants (Grant Nos. MOE2018-T2-1-076 and MOE2017-T2-2-011).

DATA AVAILABILITY

The data that support the findings of this study are available from the corresponding author upon reasonable request.

REFERENCES

[1]M. I. Dyakonov and V. I. Perel, Phys. Lett. A **35**, 459 (1971).
[2]J. E. Hirsch, Phys. Rev. Lett. **83**, 1834 (1999).
[3]S. Zhang, Phys. Rev. Lett. **85**, 393 (2000).
[4]A. Hoffmann, IEEE Trans. Magn. **49**, 5172 (2013).
[5]Y. A. Bychkov and É. I. Rashba, JETP Lett. **39**, 78 (1984).
[6]V. M. Edelstein, Solid State Commun. **73**, 233 (1990).
[7]J. C. Rojas Sánchez, L. Vila, G. Desfonds, S. Gambarelli, J. P. Attané, J. M. De Teresa, C. Magén, and A. Fert, Nat. Commun. **4**, 2944 (2013).
[8]V. P. Amin and M. D. Stiles, Phys. Rev. B **94**, 104419 (2016).
[9]V. P. Amin and M. D. Stiles, Phys. Rev. B **94**, 104420 (2016).
[10]V. P. Amin, J. Zemen, and M. D. Stiles, Phys. Rev. Lett. **121**, 136805 (2018).
[11]C. O. Avci, K. Garello, C. Nistor, S. Godey, B. Ballesteros, A. Mugarza, A. Barla, M. Valvidares, E. Pellegrin, A. Ghosh, I. M. Miron, O. Boulle, S. Auffret, G. Gaudin, and P. Gambardella, Phys. Rev. B **89**, 214419 (2014).
[12]K. Garello, I. M. Miron, C. O. Avci, F. Freimuth, Y. Mokrousov, S. Blügel, S. Auffret, O. Boulle, G. Gaudin, and P. Gambardella, Nat. Nanotechnol. **8**, 587 (2013).
[13]A. Manchon and S. Zhang, Phys. Rev. B **79**, 09442 (2009).
[14]N. Nagaosa, J. Sinova, S. Onoda, A. H. MacDonald, and N. P. Ong, Rev. Mod. Phys. **82**, 1539 (2010).
[15]T. Taniguchi, J. Grollier, and M. D. Stiles, Phys. Rev. Appl. **3**, 044001 (2015).
[16]A. Bose, D. D. Lam, S. Bhuktare, S. Dutta, H. Singh, Y. Jibiki, M. Goto, S. Miwa, and A. A. Tulapurkar, Phys. Rev. Appl. **9**, 064026 (2018).
[17]J. D. Gibbons, D. MacNeill, R. A. Buhrman, and D. C. Ralph, Phys. Rev. Appl. **9**, 064033 (2018).
[18]S. Iihama, T. Taniguchi, K. Yakushiji, A. Fukushima, Y. Shiota, S. Tsunegi, R. Hiramatsu, S. Yuasa, Y. Suzuki, and H. Kubota, Nat. Electron. **1**, 120 (2018).
[19]T. Seki, S. Iihama, T. Taniguchi, and K. Takanashi, Phys. Rev. B **100**, 144427 (2019).
[20]T. Taniguchi, AIP Adv. **8**, 055916 (2018).
[21]Z. Luo, Q. Zhang, Y. Xu, Y. Yang, X. Zhang, and Y. Wu, Phys. Rev. Appl. **11**, 064021 (2019).
[22]V. Zayets, Phys. Rev. B **86**, 174415 (2012).
[23]J. Kessler, *Polarized Electrons*, 2nd ed. (Springer, Berlin Heidelberg, 1985).
[24]Y. Xu, Y. Yang, Z. Luo, and Y. Wu, Phys. Rev. B **100**, 094413 (2019).
[25]X. Fan, J. Wu, Y. Chen, M. J. Jerry, H. Zhang, and J. Q. Xiao, Nat. Commun. **4**, 1799 (2013).
[26]X. Fan, H. Celik, J. Wu, C. Ni, K. J. Lee, V. O. Lorenz, and J. Q. Xiao, Nat. Commun. **5**, 3042 (2014).
[27]S. Emori, T. Nan, A. M. Belkessam, X. Wang, A. D. Matyushov, C. J. Babroski, Y. Gao, H. Lin, and N. X. Sun, Phys. Rev. B **93**, 180402(R) (2016).
[28]Y. Yang, Y. Xu, H. Xie, B. Xu, and Y. Wu, Appl. Phys. Lett. **111**, 032402 (2017).
[29]Y. Xu, Y. Yang, Z. Luo, B. Xu, and Y. Wu, J. Appl. Phys. **122**, 193904 (2017).
[30]Y. Xu, Y. Yang, M. Zhang, Z. Luo, and Y. Wu, Adv. Mater. Technol. **3**, 1800073 (2018).
[31]B. Wang, Y. Guo, B. Han, Z. Yan, T. Wang, D. Yang, X. Fan, and J. Cao, Appl. Phys. Lett. **116**, 222402 (2020).
[32]Y. Yang, Z. Luo, H. Wu, Y. Xu, R. W. Li, S. J. Pennycook, S. Zhang, and Y. Wu, Nat. Commun. **9**, 2255 (2018).
[33]C. O. Avci, K. Garello, M. Gabureac, A. Ghosh, A. Fuhrer, S. F. Alvarado, and P. Gambardella, Phys. Rev. B **90**, 224427 (2014).
[34]C. O. Avci, K. Garello, A. Ghosh, M. Gabureac, S. F. Alvarado, and P. Gambardella, Nat. Phys. **11**, 570 (2015).
[35]M. Hayashi, J. Kim, M. Yamanouchi, and H. Ohno, Phys. Rev. B **89**, 144425 (2014).
[36]H. Zhang, F. Freimuth, S. Blügel, Y. Mokrousov, and I. Souza, Phys. Rev. Lett. **106**, 117202 (2011).
[37]V. P. Amin, J. Li, M. D. Stiles, and P. M. Haney, Phys. Rev. B **99**, 220405(R) (2019).
[38]P. M. Haney and M. D. Stiles, Phys. Rev. Lett. **105**, 126602 (2010).
[39]A. Davidson, V. P. Amin, W. S. Aljuaid, P. M. Haney, and X. Fan, Phys. Lett. A **384**, 126228 (2020).
[40]G. Qu, K. Nakamura, and M. Hayashi, arXiv:1901.10740 (2019).
[41]C. O. Pauyac, M. Chshiev, A. Manchon, and S. A. Nikolaev, Phys. Rev. Lett. **120**, 176802 (2018).
[42]M. Kimata, H. Chen, K. Kondou, S. Sugimoto, P. K. Muduli, M. Ikhlas, Y. Omori, T. Tomita, A. H. MacDonald, S. Nakatsuji, and Y. Otani, Nature **565**, 627 (2019).
[43]D. Tian, Y. Li, D. Qu, S. Y. Huang, X. Jin, and C. L. Chien, Phys. Rev. B **94**, 020403(R) (2016).
[44]K. S. Das, W. Y. Schoemaker, B. J. van Wees, and I. J. Vera-Marun, Phys. Rev. B **96**, 220408(R) (2017).
[45]K. S. Das, J. Liu, B. J. van Wees, and I. J. Vera-Marun, Nano Lett. **18**, 5633 (2018).
[46]Z. Zhu, X. Zheng, G. Li, H. Bai, J. Su, Y. Zhang, and J. Cai, NPG Asia Mater. **12**, 12 (2020).
[47]W. Wang, T. Wang, V. P. Amin, Y. Wang, A. Radhakrishnan, A. Davidson, S. R. Allen, T. J. Silva, H. Ohldag, D. Balzar, B. L. Zink, P. M. Haney, J. Q. Xiao, D. G. Cahill, V. O. Lorenz, and X. Fan, Nat. Nanotechnol. **14**, 819 (2019).
[48]L. Liu, J. Yu, R. González-Hernández, C. Li, J. Deng, W. Lin, C. Zhou, T. Zhou, J. Zhou, H. Wang, R. Guo, H. Y. Yoong, G. M. Chow, X. Han, B. Dupé, J. Železný, J. Sinova, and J. Chen, Phys. Rev. B **101**, 220402(R) (2020).
[49]M. Tang, K. Shen, S. Xu, H. Yang, S. Hu, W. Lü, C. Li, M. Li, Z. Yuan, S. J. Pennycook, K. Xia, A. Manchon, S. Zhou, and X. Qiu, Adv. Mater. **32**, 2002607 (2020).
[50]Q. Zhang, Z. Luo, H. Li, Y. Yang, X. Zhang, and Y. Wu, Phys. Rev. Appl. **12**, 054027 (2019).